# Studies of Pinch Dynamics and Fusion-Products Emission within a Mega-Joule Plasma-Focus Facility

M. Scholz, B. Bienkowska, I.M. Ivanova-Stanik, L. Karpinski, M. Paduch, W. Stepniewski
E. Zielinska, J. Kravarik*, P. Kubes*, A. Malinowska**, M.J. Sadowski *&**), A. Szydlowski**)

*Institute of Plasma Physics and Laser Microfusion (IPPLM), 23 Hery, 03-908 Warsaw, Poland*
*Phone: +48 22 7180611, Fax: +48 22 7793481, E-mail:mareki@ifpilmj.waw.pl*
** Czech Technical University (CVUT), Technicka 2, 166-27 Prague, Czech Republic*
***The Andrzej Soltan Institute for Nuclear Studies (IPJ), 05-400 Otwock-Swierk, Poland,*

**Abstract – The paper concerns emission characteristics of high-current discharges, studied in the mega-joule PF-1000 facility operated at IPPLM. Particular attention was paid to studies of a detailed sequence of emission phenomena within individual discharges. Measurements performed within the PF-1000 device determined the temporal correlation of X-rays and neutrons. Using the TOF technique, it was estimated that energy of fusion-neutrons in the dominant peak, measured at $\theta = 0^0$ and $180^0$, was 2.69 and 2.14 MeV with energy resolution equal to about 13%. The two-pulse neutron emission was compared with the visible-radiation pictures taken with micro-channel plates in the PF-1000 facility. Effects of the shortening of a pinch plasma column and the formation of dense spherical structures were observed.**

## 1. Introduction

Dense Plasma-Focus devices are high-voltage discharge facilities, which belong to Z-pinches and can produce hot plasma and intense radiation pulses (neutrons, X-rays, electron- and ion-beams). In a consequence, it leads to the generation of powerful beams of electrons and ions as well as the intense emission of X-rays and fusion neutrons and protons (when the filling gas is deuterium) [1-3]. To investigate the neutron generation and to define the temporal-correlation among neutron-, X-ray- and electron-peaks, several new series of measurements have recently been performed within the PF-1000 device. The X-ray and neutron pulses were measured with scintillation detectors. The fast electron beams were measured with Cerenkov-type detectors located upstream and downstream the electrode system. Those detectors contained rutile crystals covered with Cu-foils of different thickness, and they were coupled with fast photomultipliers. Signals from the Cerenkov detectors, as recorded with a fast oscilloscope, were correlated with signals from other diagnostic tools. Electron beam signals were compared with soft- and hard-X-rays as well as neutron pulses. Dynamics of a current-sheath was studied with fast-streak cameras. The four-frame camera recorded the visible radiation and another four-frame one observed soft X-ray range. It was observed that motion of the current sheet had a complicated two-dimensional character. After the axial acceleration-phase it changed rapidly in the radial compression.

Time-resolved X-ray signals, as measured with PIN-diodes covered with different filters, were compared with other traces (voltage-waveforms, dI/dt signals and neutron-induced pulses). The total neutron yield ($Y_{tot}$), as produced during a single discharge and emitted in various directions, was measured with several silver-activation detectors placed at different angles around the PF-1000 vacuum chamber. To perform time-resolved measurements of hard X-rays and fusion-neutrons, we used six scintillation probes, which were located on z-axis of the PF electrodes (at $0^o$ and $180^o$). The main aims of the recent experiments were as follows:

1. The determination of characteristics of fusion-products (fast neutrons and protons), i.e. their spatial- and temporal-distributions, anisotropy, and contributions of different production mechanisms;
2. The investigation of the relation between the total neutron yield and plasma-sheath dynamics, with particular attention paid to structures appearing within the pinch-column.

## 2. Experimental set-ups and diagnostics

The measurements were performed within the PF-1000 plasma-focus facility having the maximum bank energy of about 1.2 MJ. The facility had the Mather-type electrode configuration. A copper anode was 231 mm in diameter and 600 mm in length. The cylindrical alumina insulator (embracing the anode) was 113 mm in length. The outer electrode consisted of a 12 stainless steel tubes of 80 mm in diameter. Hence, the inter-electrode gap was 44.5 mm. The facility was operated under the same conditions during each shot, i.e. the initial filling deuterium pressure was p = 4.655 hPa, charging voltage of the condenser bank was $U_0$ = 27 kV, and bank energy amounted to $W_0$ = 480 kJ. The external inductance of the circuit was $L_0$ =10 nH. The maximum amplitude of the discharge current was about 1.8 – 1.9 MA, and its rise time was 7.5 μs, as

measured with a good repeatability by means of a Rogowski coil.

In order to measure the total neutron yield and neutron angular distribution at the PF-1000 facility, there were designed and manufactured five silver-activation counters. The neutron yields were measured at different angles to the z-axis, i.e. at $30^0$, $60^0$, $90^0$ and $150^0$. The counters (SC1 – SC5) were placed around the main PF-1000 discharge chamber, as shown in Fig. 1.

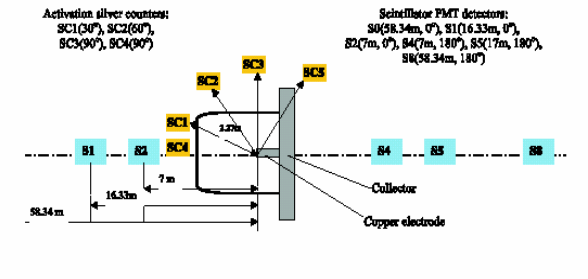


Fig.1. Location of the neutron detectors

Six scintillation probes were applied to perform detailed time-resolved (TOF) measurements of the neutron emission and hard X-rays, which penetrated steal- or lead-shields of 3–5 cm in thickness. The probes (S1 – S6) were equipped with NE-102 detectors coupled with fast photo-multipliers. The described probes were located at an angle $\varphi = 0^0$ at distances of 7.0 m, 16.3 m and 58.3 m from the center of the electrode outlet, and at the angle $\varphi = 180^0$ at distances of 7.0 m, 16.3 m and 58.3 m (as shown in Fig.1). Within the PF-1000 facility those angles corresponded to measurements in the downstream (along the z-axis) and upstream (in the opposite direction), respectively.

The evolution of a PF current sheath and pinch dynamics were studied by means of optical frame- and streak-cameras. The three-frame camera was placed side-on the PF-1000 facility. Depending on the measurement series, a time delay between subsequent frames was 10 ns or 20 ns. An interference filter ($\lambda_{max}$ = 593 nm, FWHM = 6 nm) was located in the optical path of the passive optical diagnostic subsystem. Its spectral characteristics enabled to record only intensity of the continuous radiation.

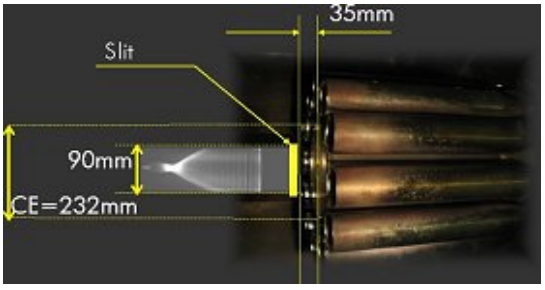


Fig.2. Electrode outlets and high-speed smear photo

The time resolving streak camera, which operated within the spectral range of 700-900 nm, observed the PF pinch region perpendicularly to the z-axis. The location of the input slit (of about 0.1 mm in width) in relation to the electrode outlets, and an example of the smear picture have been shown in Fig. 2.

## 3. Experimental results

Typical sequences of the frame pictures, which were taken in the visible wavelength range during the operation of the PF-1000 device at the same initial condition and with similar neutron yields, are presented in Fig. 3.

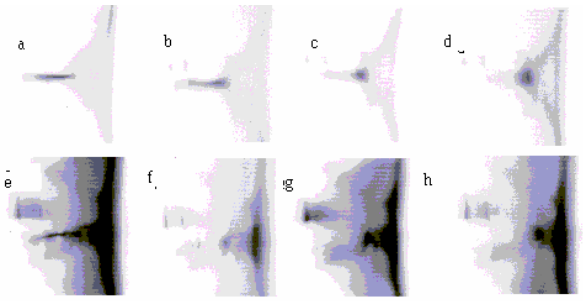


Fig.3. High-speed frame pictures recorded for 2 shots (#4618 and #5055) within the PF-1000 experiment

It was assumed that $t = 0$ corresponds to the instant when the peak of soft x-rays appears, and the narrow radiating pinch column of about 5 mm in diameter and 5 cm in length is observed, as shown in Fig. 3a. This pinch phase was ended by the creation of a dense spherical structure of ~ 1 cm in diameter (shown in Fig.3d). That spherical structure was formed at a distance of about 6-8 cm from the anode end, at the top of the focus region and at the bottom of the dilated current sheath.

It should be noted that the second pinch, i.e. the radial implosion of the week radiating region, which surrounded dark zones (of low temperature and density) was also observed (see Figs 3e-3h). During the considered phase the pinch diameter decreased considerably, but intensity of the emitted radiation increased.

The later explosion of the second pinch was probably very fast and it was not recoded upon the obtained frame images. There was recorded only the dense structure formed at a distance of about 8 cm (in front of the anode), at the bottom of the dilated current sheath. It was similar to the structure recorded after the first pinch (shown in Fig.3d). The evolution of the pinch phase, which was recorded upon the presented frames, was observed in the period of the neutron production. At later instants $t$ = 120-130 ns the hot and dense second pinch column was formed in the correla-

tion with the second implosion, as one can easily observe in the streak-camera picture shown in Fig. 4.

Typical signals of the instantaneous X-rays and fast fusion neutrons, as recorded by the scintillation probes placed at a distance 58.3 m, at the angles of $0^0$ and $180^0$ to the pinch axis, are presented in Fig.5.

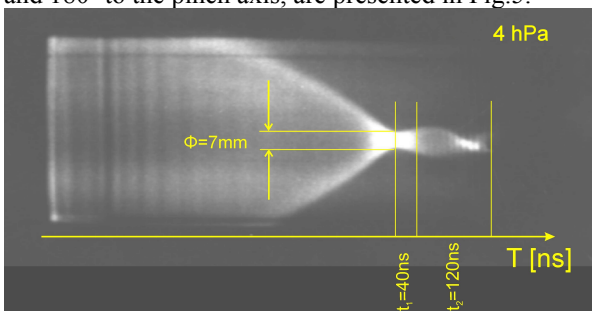


Fig.4. High-speed smear picture showing the formation of the second pinch (shot #5055)

Energy values, which corresponded to the peak of the neutron TOF signal measured at the angles of $0^0$ and $180^0$, were denoted as E(0) and E(180), respectively. On the basis of the described measurements the average values of the maximum energy of fusion neutrons was found to be E(0) = 2.69 MeV and E(180) = 2.14 MeV, correspondingly.

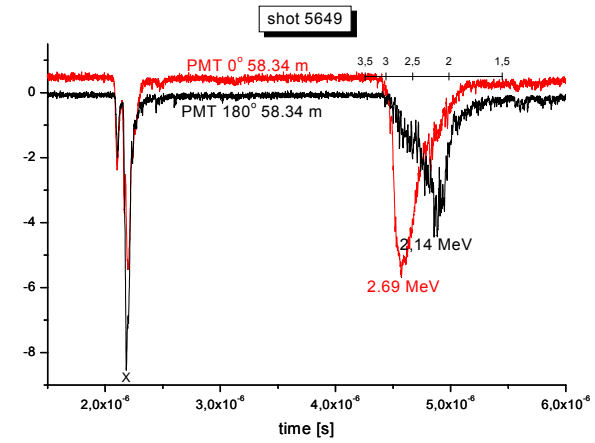


Fig.5. X-ray and fusion-neutron signals recorded at the same distance but at different angles to the z-axis

The neutron signals were also compared with other waveforms, as shown in Fig. 6. One can easily observe that the recorded neutron signals had the double peak structure, with the second pulse more intense than the first one, in contrary to observations in other PF-type devices. Analyzing the traces presented in Fig. 6 one can observe that the first maximum of the neutron signal $Y(t)$ appeared about 323 ns after the PIN-diode signal dip. This time interval exactly corresponds to the time-of-flight of 2.45 MeV neutrons from the pinch to the used scintillation detector. The second maximum of the neutron signal correlates with the second relatively lower soft X-ray (SXR) pulse as well as with the hard X-ray signals and the electron beam pulse.

To investigate fast ion beams emitted from the pinch column several samples of nuclear track detectors (NTD) were irradiated during a single PF-1000 shot, which was performed with the $D_2$ filling. After the irradiation those samples were etched under standard conditions and scanned with an optical microscope. The optical analysis has shown that the ion crater surface densities ranged from $10^3$–$10^5$ tracks/mm$^2$ up to the full saturation level. To interpret those results we took into account energy losses of $D^+$-ions in Al absorption foils which covered the NTD (e.g. $D^+$-ions of energy > 250 keV could penetrate through 1.5-μm Al-foil, and 500-keV ions - through a 4-μm Al-foil), as well as the detection characteristics of the detectors applied [4, 5]. Hence, one could estimate that the uncovered NTD recorded $D^+$-ions of energy above 80 keV, while the detectors covered by a 1.5-μm Al foil registered $D^+$-ions of energies above 330 keV, and samples shielded with a 4-μm Al foil revealed tracks of ions of energies > 580 keV. It was, however, observed that the emission of such fast ions was not reproducible from shot to shot, and it was less reproducible that the neutron emission. Nevertheless, its absolute yield decreased with an increase in the filling pressure, as usually.

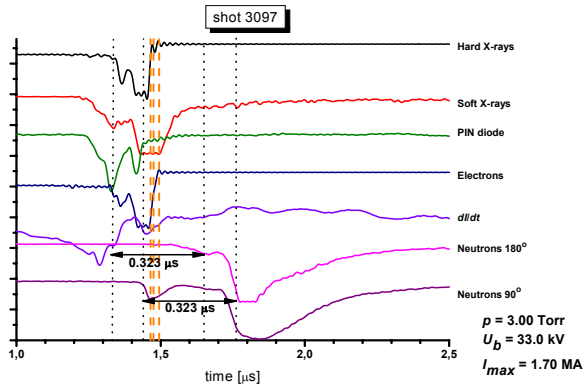


Fig.6. Comparison of waveforms (from top to bottom) corresponding hard X-rays, soft X-rays, PIN-diode signal, electron signal, dI/dt and neutron signals)

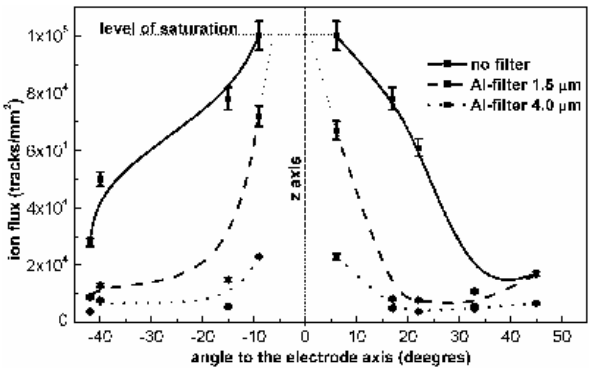


Fig.7. Angular distributions of fast deuterons

The angular distributions of accelerated primary deuterons (of different energies), as obtained from a single PF-1000 shot performed at the filling pressure of 1.9 Torr $D_2$, are presented in Fig. 7. It should be noted that the central parts (near Z-axis) of the NTDs was usually damaged, in spite of their relatively big distances from the pinch region.

## 4. Discussion of results and conclusions

The investigation of processes of the creation and disruption of the pinch column demonstrated that two pinches occur during that phase of the PF discharge (see Fig.4). From the streak camera images obtained for discharges with similar neutron yields, it was learned that time intervals, life-time of the pinch and its dimension strongly depends on the deuterium filling pressure. It was also found that time intervals between pinches depend on the total neutron yield for shots at the same pressure. At larger neutron yields this time interval decreases. If no neutron yield is recorded, the second pinch is also not observed. One of interpretations of that phenomenon could be based on the relationship between the neutron production and the current flowing through plasma (neglecting the axial outflow of the current from the pinch column). In the case of a high current the accompanying magnetic field exerts a high pressure on plasma, and it does not allow the long-lasting free expansion of the pinch. As a result, it causes the fast second pinch, which is observed as two luminous regions close each other on the streak images. When the current and neutron yield are low, a weak magnetic field does not balance plasma pressure until plasma particle concentration decreases strongly enough, i.e. until the expanding pinch increases its dimensions considerably. As a result, the second pinch can occur after much longer time. Comparing the obtained streak images with other diagnostic signals, it can be stated that hard X-ray radiation pulse is usually generated during the first pinch (in most discharges), while the soft X-ray pulse is emitted during the first and the second pinch, as shown in Fig. 8.

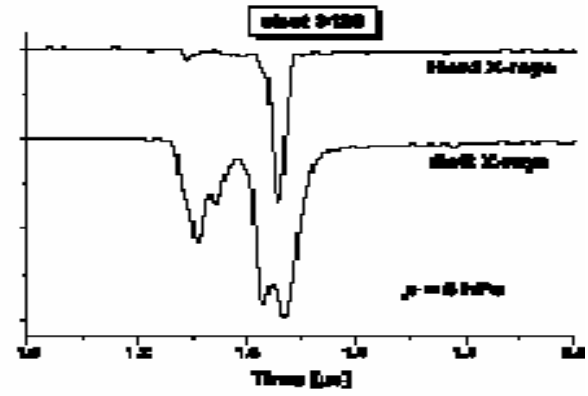

Fig.8. Comparison of hard and soft X-ray pulses

It should be noted that there were also PF shots in which the hard X-ray pulse was correlated with second pinch, particularly when neutron yield was high. Taking into account that the neutron energy values observed downstream and upstream were different (see Fig.5), one should consider models including motion of the center–of–mass (c.m.). Motion of the c.m. can arise in the beam-target model or in a model in which portion of plasma ions undergoes movement with velocity $v_{cm}$ along the axis (a moving isotropic plasma model). Since our optical and neutron observations of the plasma axial motion indicated velocities of about $10^8$ cm/s, the c.m. velocity equal to about $1.3 \cdot 10^8$ cm/s seems to be a realistic one. It suggests that the moving-plasma model agrees better with our experimental data. However, three or two peaks in the hard X-ray signals and the fine structure of the neutron-induced signals (see Fig 9.) were observed in many PF-1000 shots. It suggests that two or three pulses of fast neutrons with different maximum energy values can be emitted from the PF-1000 pinch column.

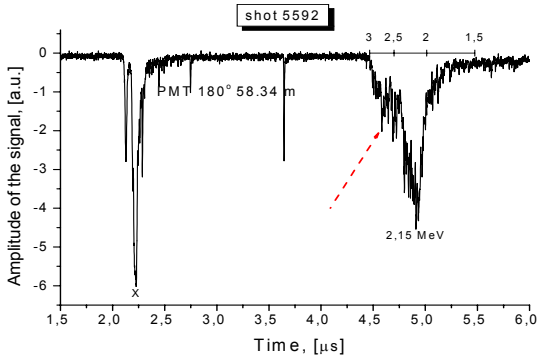


Fig.9. Fine structure of the X-ray and neutron signals

The results of the reported measurements made possible to compare the moving plasma model and the beam–target model. Nevertheless, the real physical mechanisms, inducing the ion acceleration and specific properties of the main (well-localized) neutron source, are still unknown. However, the summary of the results obtained in the described PF-1000 experiment suggest a more sophisticated model, e.g. that similar to the gyrating-particle model [6].

## References

[1] J.W. Mather, *in Methods of experimental physics,* Ed. by R.H. Lovberg, H.R. Griem, Vol. 9, Acad. Press, New York – London 1971, pp. 187-249.
[2] J.W. Mather, Phys. Fluids Suppl. **7** (1964) 528.
[3] A. Bernard, H. Bruzzone, P. Choi, et al., J. Moscow Phys. Soc. **8** (1998) 1.
[4] M. Sadowski, E. Al-Mashhadani,, A. Szydlowski, et al., Nucl. Inst Meth. **B 86** (1994) 311.
[5] A. Szydlowski, M. Sadowski, T. Czyzewski, et al., Nucl. Inst Meth. **B 149** (1999) 113.
[6] U. Jager, H. Herold, Nuclear Fusion **27** (1987) 407.